Journal of the Serbian Chemical Society
JSCS-info@shd.org.rs • www.shd.org.rs/JSCS

J. Serb. Chem. Soc. 76 (10) 1365–1378 (2011)
JSCS–4211

UDC 546.656+577.213.3+
547.963.32:615.2:537.87
Original scientific paper

Mechanisms of the interaction between $Pr(DNR)_3$ and herring-sperm DNA

XIAOCAI LIU[1], XINGMING WANG[1]* and LISHENG DING[2]

[1]*School of Materials Science and Engineering, Southwest University of Science and Technology, Mianyang 62101 and* [2]*Chengdu Institute of Biology, Chinese Academy of Sciences, Chengdu 610041, China*

(Received 26 August, revised 8 November 2010)

Abstract: Research on the interaction mechanism of drugs with DNA is essential to understand their pharmacokinetics. The interaction between rare earth complexes $Pr(DNR)_3$ and herring-sperm DNA was studied in Tris-HCl buffer solution (pH 7.4) by absorption and fluorescence spectroscopy and viscosity measurements. The results showed that the modes of interaction between $Pr(DNR)_3$ and herring-sperm DNA were electrostatic and intercalation. The binding ratio was $n_{Pr(DNA)_3}$: n_{DNA} = 5:1 and the binding constant was $K^{\ominus}$(292 K) = 4.34×10^3 L mol^{-1}. Furthermore, according to the double reciprocal method and the thermodynamic equation, the intercalative interaction was cooperatively driven by an enthalpy effect and an entropy effect.

Keywords: daunorubicin; rare earth complexes; herring-sperm DNA; acridine orange; interaction mechanism.

INTRODUCTION

Drug therapy is currently one of the main means of combating cancer; therefore, the design of anti-cancer drugs is mostly based on DNA as the target. The study of the mechanism of drugs and DNA interaction has important significance in the synthesis of anti-cancer drugs.[1] Drugs binding to DNA have been studied by numerous researchers.[2,3]

Daunorubicin (DNR) (Fig. 1) is a clinically used antitumor anthracycline antibiotic.[4–6] Its anticancer activity is due to the formation of intercalative complexes with DNA and inhibition of the duplication of both DNA and RNA. However, its side effects, especially its cardiotoxicity, have greatly restrained its application.[7] A great deal of research was aimed at reducing the toxicity of DNR by remodeling its structure,[8–11] and by forming metal ion–DNR complexes to protect the quinone structure from being reduced.[12–14]

* Corresponding author. E-mail: xmwang_xkd@yahoo.com.cn
doi: 10.2298/JSC100826121L

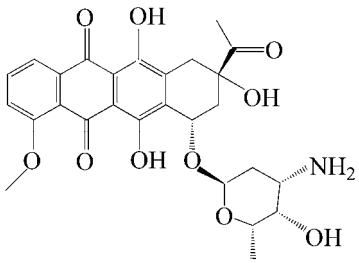

Fig. 1. The structure of DNR.

However, the complexes formed between anthracycline antibiotics and rare earth metals with pharmacological activity have not been researched for anti-cancer applications. In the present study, $Pr(DNR)_3$ complexes were synthesized and then attention was focused on the mechanism of interaction of $Pr(DNR)_3$ with DNA. It was expected that the results could be of significance in the fields of the chemistry of rare earth complexes, biological inorganic chemistry and drug inorganic chemistry.[15,16]

EXPERIMENTAL

Instruments and reagents

Herring-sperm DNA (hs-DNA) and DNA bases were purchased from Sigma Biological Co. and used as received. Acridine orange (AO) was purchased from Shanghai-China Medicine Chemical Plant (A.R.). Pr_2O_3 was purchased from Chengdu-China Kelong Chemical Plant (A.R.). Daunorubicin hydrochloride (DNR) was purchased from JiNan Wedu Industrial Co., Ltd., Tris-HCl buffer (pH 7.40) was used to control the pH of the reaction system. All the samples were dissolved in the Tris-HCl buffer. Other reagents were of at least analytical grade. Solutions in buffer were freshly prepared immediately before use.

The absorption spectra were recorded on an UV-210 spectrophotometer and the fluorescence spectra on a FL-4500 spectrofluorophotometer (Shimadzu, Japan). The infrared absorption spectra were recorded on FT-IR spectrometer (PE Instruments, USA). Elementary analyses were performed on a Vario EL CUBE elementary analyzer (Element Analysis System Inc., Germany). The pH was recorded on a pHS-2C acidometer (Fangzhou Technology Co., China).

Preparation of $PrCl_3$ solutions

Pr_2O_3 was dissolved in concentrated hydrochloric acid and then the solution was heated to remove the excess water and hydrochloric acid to give $PrCl_3$ as a white powder. $PrCl_3$ solutions of different concentrations were prepared in 0.10 mol L^{-1} Tris-HCl buffer solution (pH 7.4).

Synthesis of the $Pr(DNR)_3$ complex

The complex was prepared from stoichiometric amounts (1:3) of praseodymium chloride and DNR in absolute ethanol. The reaction system was recirculated on a water bath at 343 K for 12 h whereby the color of the solution changed from red to red-brown. The sample was concentrated to 10 mL in an oven for 5 h. During standing for several days, a brownish precipitation of $Pr(DNR)_3$ formed.

The $Pr(DNR)_3$ complex was characterized by elemental analysis and IR spectroscopy.

The absorption spectra and fluorescence spectra

A solution of $Pr(DNR)_3$ (1.17×10^{-5} mol L^{-1}, 3 mL) in Tris-HCl buffer (pH 7.4) was titrated in a 1 cm pathlength cuvette by adding successively 10 μL of a DNA solution (1.00×10^{-4} mol L^{-1}). After each addition, the absorption and fluorescence spectra were recorded. Tris-HCl buffer solution served as the reference for the absorption measurements. The excitation wavelength for the fluorescence measurements was 411.7 nm and the excitation and emission slits were both set at 10 nm. The volume effect was so small that it could be ignored. Additionally, AO was used as a fluorescent probe to study the interaction mode between the complex and DNA.

Viscosity measurements

Viscosity measurements were performed using a Ubbelohde viscometer, which was immersed in a thermostat water-bath at room temperature. Different amounts of $Pr(DNR)_3$ (1.0×10^{-6}–5.0×10^{-6} mol L^{-1}) were added into the viscometer while keeping the DNA concentration constant at 1.00×10^{-5} mol L^{-1}. The flow time of the samples was repeatedly measured with an accuracy of ±0.20 s using a digital stopwatch. The flow times were above 250 s and each point represents the average of at least three readings. The data is presented as $(\eta/\eta_0)^{1/3}$ *vs.* $c_{Pr(DNR)_3}$, where η and η_0 are the relative viscosities of the DNA solution in the presence and absence of the $Pr(DNR)_3$ complex, respectively.

RESULTS AND DISCUSSION

Characterization of the $Pr(DNR)_3$ complex

In contrast to DNR (data in parentheses), the IR spectrum of $Pr(DNR)_3$ displayed clearly the stretching vibration band of OH at 3428 cm^{-1} (ν_{OH} = 3443 cm^{-1}). The bending vibration of $–CH_2–$ was at 2931 cm^{-1} (ν_{CH} = 2919 cm^{-1}). The stretching vibration band of the CN and the bending vibration of NH were at 1273 cm^{-1} ($\nu_{CN} + \delta_{NH}$ = 1292 cm^{-1}). The stretching vibration band of CN was at 1115 cm^{-1} (ν_{CN} = 1126 cm^{-1}). These results show that the bands in the IR spectrum of the complex (OH, CN and NH) were shifted to lower frequencies in comparison to the corresponding bands in the spectrum of DNR. This proves the formation of the Pr–DNR complex.

Elemental analysis. C, 51.68; H, 5.29; N, 2.28 % (experimental data). C, 53.17; H, 4.79; N 2.30 % (theoretical value).

From the results of the elemental analysis, the formula of the complex was speculated as $[Pr(C_{27}H_{29}NO_{10})_3]Cl_3$.

Determination of the binding ratio of Pr^{3+} and DNR using the mole ratio method

Fluorescence spectra were obtained by titration of a $PrCl_3$ solution with increasing concentrations of DNR (Fig. 2). With the addition of DNR, the intensity of the fluorescence peak at 593 nm decreased gradually. The experiment results indicated that there was an interaction between Pr^{3+} and DNR, leading eventually to the formation of the Pr–DNR complex.

In order to determine the stoichiometry of the complex, the mole ratio method was employed using the intensity of the fluorescence peak at 593 nm (Fig. 3). The binding ratio[17] of DNR and Pr^{3+} was obtained as n_{Pr}:n_{DNR} = 1:3.

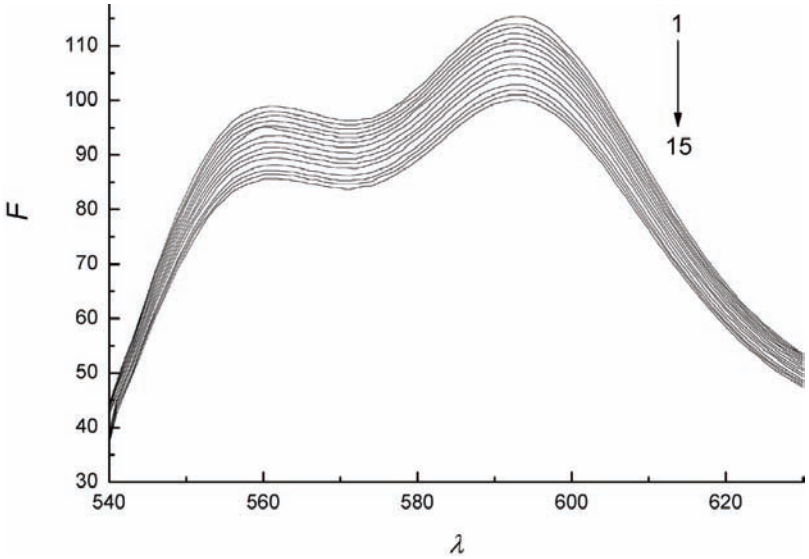

Fig. 2. The emission spectra of DNR in different concentrations of Pr^{3+}; c_{DNR} = 2.00×10^{-5} mol L^{-1}, c_{Pr} = 2.68×10^{-4} mol L^{-1} (10 μL per scan); λ in nm.

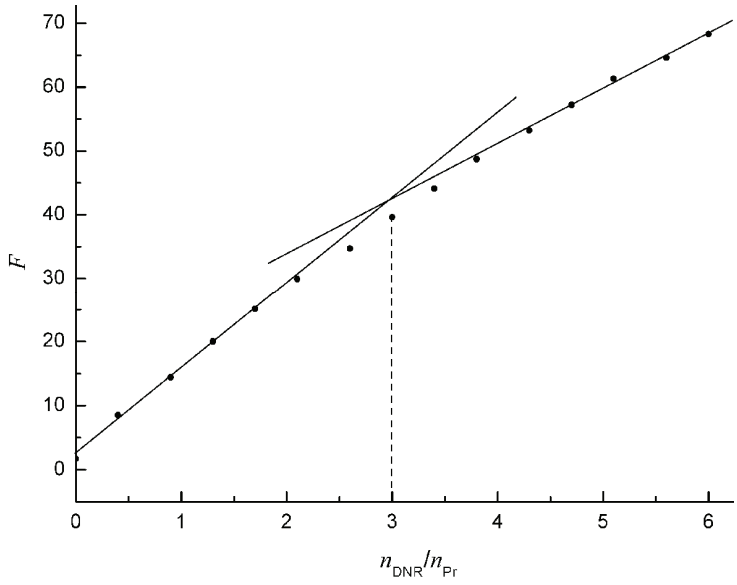

Fig. 3. Mole ratio method. c_{DNR} = 2.00×10^{-4} mol L^{-1} (10 μL per scan), c_{Pr} = 1.56×10^{-6} mol L^{-1}.

The fluorescence spectra of $Pr(DNR)_3$ complex and DNA

With a fixed concentration of $Pr(DNR)_3$ complex, the concentration of DNA was stepwise increased and after each step, the fluorescence emission spectrum of the system was recorded (Fig. 4). The results show that with increasing DNA concentration, the fluorescence intensity of $Pr(DNR)_3$ gradually decreased, *i.e.*, the fluorescence of $Pr(DNR)_3$ was quenched by DNA. This indicates that there was interaction between DNA and $Pr(DNR)_3$.

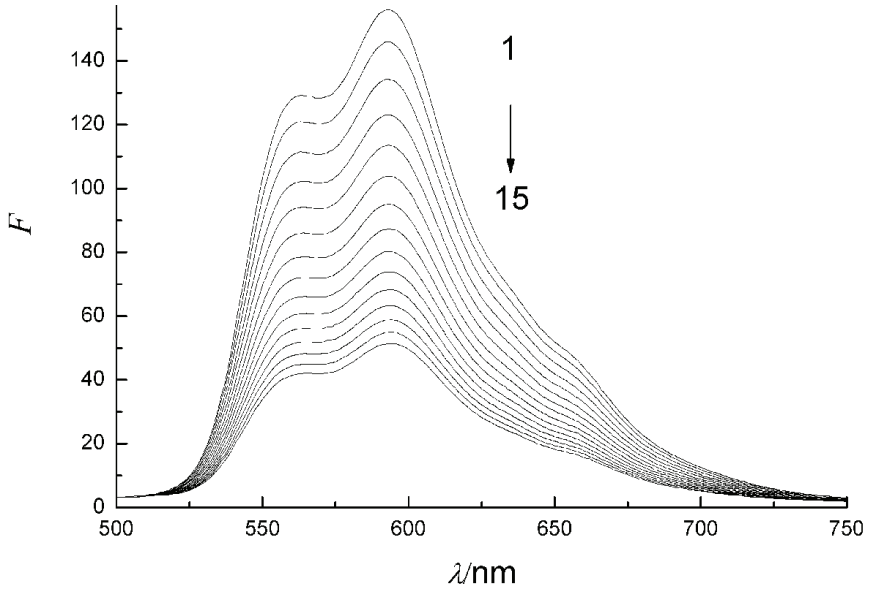

Fig. 4. Fluorescence spectra of the complex in the presence of different concentrations of DNA; $c_{Pr(DNR)_3} = 1.17\times10^{-5}$ mol L^{-1}, $c_{DNA} = 1.00\times10^{-4}$ mol L^{-1} (10 μL per scan).

The electronic absorption spectra of $Pr(DNR)_3$ complex and DNA

UV–Vis spectroscopy is the most common and convenient way to study interactions between small molecules or rare earth complexes and nucleic acid.

The double helix structure of DNA molecules contains aromatic base and phosphate chromophore groups, therefore, interactions between the small molecules and DNA can be studied according to changes in the absorption spectra before and after reaction.

A red shift (or blue shift), hyperchromic (hypochromic) effect, and the isochromatic point are spectral properties of DNA which are closely related with the double helix structure.[18] Generally, a red shift (or blue shift) and a hypochromic (or hyperchromic) effect[19] are observed in the absorption spectra if small molecules intercalate with DNA. A hypochromic effect will be obvious if the intercalation is strong.[20] A red shift and a hypochromic effect are not obvious in the

absorption spectra if the interaction mode of the small molecules with DNA is electrostatic or groove binding.

With a fixed concentration of $Pr(DNR)_3$ complex, the concentration of DNA was gradually increased and after each step, the UV–Vis spectrum of the system was recorded (Fig. 5). The results show that, with increasing DNA concentration, the absorbance of solution regularly decreased, an isochromatic point appeared at 548 nm and the maximum absorption peak was red shifted (from 479 to 502 nm). These phenomena indicate that $Pr(DNR)_3$ had interacted with DNA in the intercalation mode.

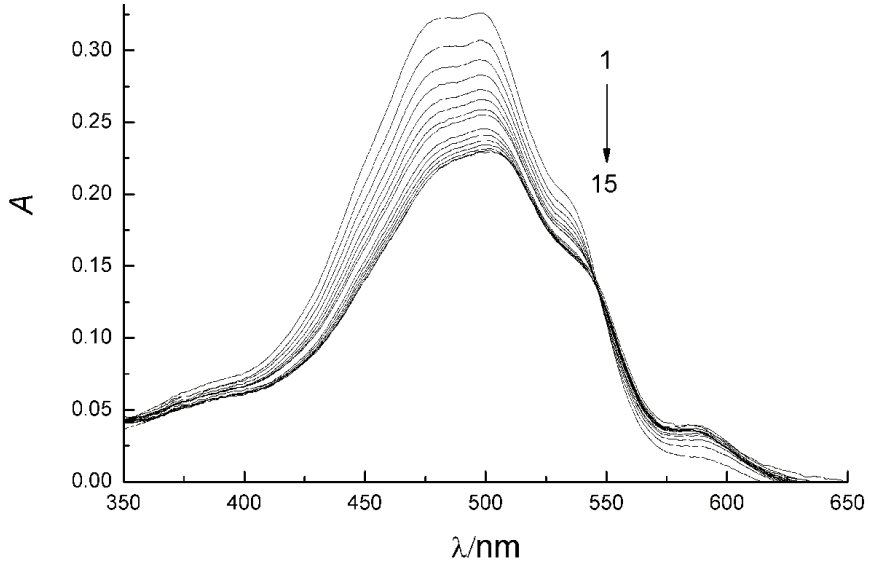

Fig. 5. Electronic absorption spectra of the complex in the presence of different concentrations of DNA; $c_{Pr(DNR)_3} = 1.17\times10^{-5}$ mol L^{-1}, $c_{DNA} = 1.00\times10^{-4}$ mol L^{-1} (10 μL per scan).

Determination of the binding ratio of $Pr(DNR)_3$ and DNA by the mole ratio method

To a fixed concentration of $Pr(DNR)_3$ complex in buffer solution (pH 7.40) was added DNA solution in portions. After each addition the fluorescence emission spectrum was recorded. The intensity of the fluorescence peak at 593 nm was used to determine the binding ratio by the mole ratio method (Fig. 6). The binding ratio of $Pr(DNR)_3$ and DNA of $n_{Pr(DNR)_3}$:n_{DNA} of 5:1 was obtained.

In the same manner, the electronic absorption spectra of the system after successive additions of DNA were recorded (Fig. 7) and the same binding ratio was obtained.

Determination of the binding constants and thermodynamic constants by the double-reciprocal method

In order to further understand the interaction mode of $Pr(DNR)_3$ with DNA, studies of the thermodynamics were undertaken. For this purpose, absorption spectra were recorded at 292 and 310 K. The following double-reciprocal equation was employed:[21]

$$1/(A_0 - A) = 1/A_0 + 1/(KA_0c_{DNA}) \quad (1)$$

where A_0 and A are the absorbances of $Pr(DNR)_3$ in the absence and in the presence of DNA, respectively. K is the binding constants between $Pr(DNR)_3$ and DNA and c_{DNA} is the concentration of DNA. The double reciprocal plots of $1/(A_0-A)$ *vs.* $1/c_{DNA}$ were linear (at 292 and 310 K) and the binding constants were calculated from the ratio of the intercept/slope (Fig. 8), K (292 K) = = 4.34×10^3 L mol^{-1} and K (310 K) = 3.66×10^3 L mol^{-1}.

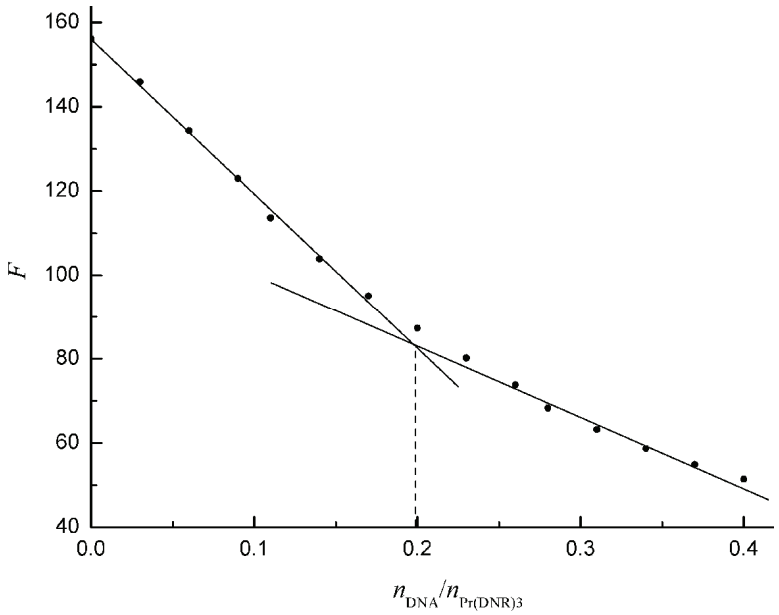

Fig. 6. Mole ratio method; $c_{Pr(DNR)_3} = 1.17\times10^{-5}$ mol L^{-1}, $c_{DNA} = 1.00\times10^{-4}$ mol L^{-1} (10 μL per scan).

The standard molar reaction Gibbs energy ($\Delta_rG_m^\ominus$) and the standard molar reaction entropy ($\Delta_rS_m^\ominus$) were estimated from the following relationships:

$$\log K^\ominus = -\Delta_rH_m^\ominus/(2.303RT) + \Delta_rS_m^\ominus/(2.303R) \quad (2)$$

$$\Delta_rG_m^\ominus = -RT\ln K^\ominus = \Delta_rH_m^\ominus - T\Delta_rS_m^\ominus \quad (3)$$

In the interaction of $Pr(DNR)_3$ and DNA, the following values were calculated: $\Delta_rH_m^\ominus = -1.35\times10^4$ J mol^{-1}, $\Delta_rS_m^\ominus = 1.12\times10^2$ J mol^{-1} K^{-1}, $\Delta_rG_m^\ominus$ (292 K) =

= -2.03×10^4 J mol^{-1} and $\Delta_r G_m^{\ominus}$ (310 K) = -2.11×10^4 J mol^{-1}. Therefore, the interaction between $Pr(DNR)_3$ and DNA could occur spontaneously. As $\Delta_r H_m^{\ominus} < 0$ and $\Delta_r S_m^{\ominus} > 0$ according to theory of thermodynamic functions, it is supposed that the intercalative interaction was cooperatively driven by an enthalpy effect and an entropy effect.[22,23]

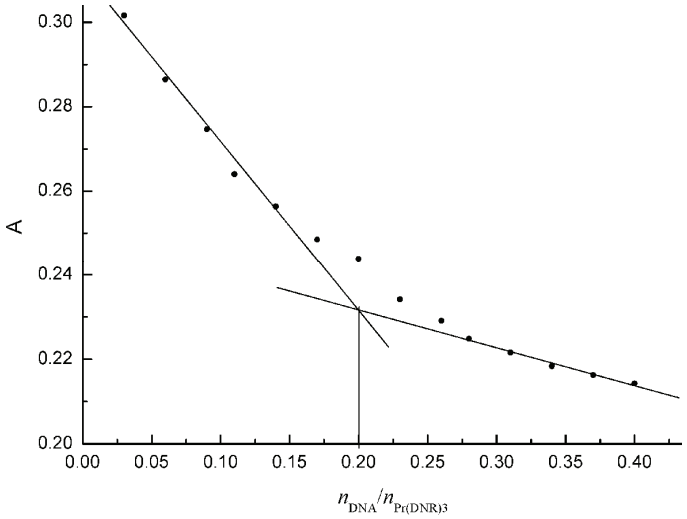

Fig. 7. Mole ratio method; $c_{Pr(DNR)_3} = 1.17\times10^{-5}$ mol L^{-1}, $c_{DNA} = 1.00\times10^{-4}$ mol L^{-1} (10 μL per scan).

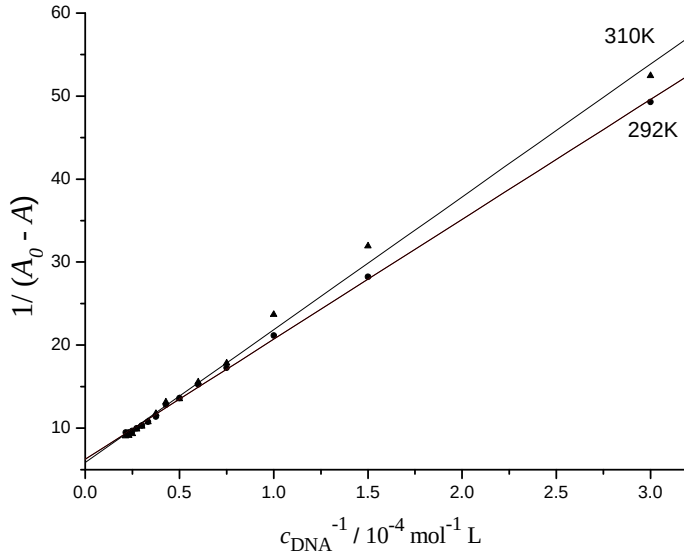

Fig. 8. Double reciprocal plots of $Pr(DNR)_3$–DNA; $c_{Pr(DNR)_3} = 1.17\times10^{-5}$ mol L^{-1}, $c_{DNA} = 1.00\times10^{-4}$ mol L^{-1} (10 μL per scan).

Fluorescence measurements using acridine orange as a probe

AO is a type of cationic dye. Due to its planar aromatic chromophore, it can insert between two adjacent base pairs in the DNA helix and significantly enhance the fluorescence. Therefore, AO is often used as a fluorescent probe to study the interaction mode between small molecules and DNA.

Influence of AO on the fluorescence spectra of Pr(DNR)$_3$–DNA

The emission spectra of Pr(DNR)$_3$–DNA in the presence of different concentrations of AO are shown in Fig. 9. With increasing concentration of AO, the fluorescence intensity of Pr(DNR)$_3$–DNA gradually increased. This showed that there was competition between AO and Pr(DNR)$_3$ for interaction with DNA and AO replaced the Pr(DNR)$_3$ which was inserted into the base pairs of the DNA.

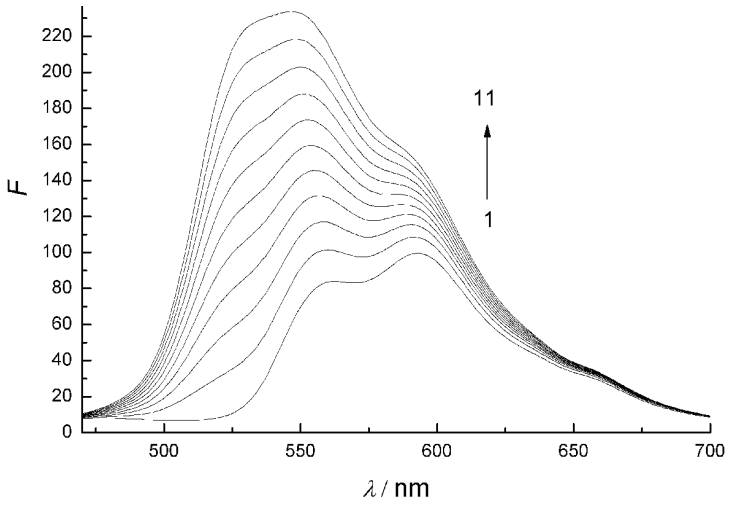

Fig. 9. Influence of AO on the emission spectra of Pr(DNR)$_3$–DNA. $c_{Pr(DNR)_3–DNA}$ = 1.00×10^{-5} mol L^{-1}, c_{AO} = 3.00×10^{-4} mol L^{-1} (10 μL per scan).

Influence on fluorescence spectra of Pr(DNR)$_3$ on AO–DNA

The fluorescence spectra of AO–DNA in the presence of different concentrations of Pr(DNR)$_3$ are shown in Fig. 10. It can be seen that the characteristic peak intensity of AO–DNA decreased and the equivalent point of the fluorescence intensity near 533 nm. These phenomena proved that AO was replaced by Pr(DNR)$_3$; hence the characteristic peak of AO–DNA was quenched. The competitive binding experiments indicated the existence of intercalation interaction.

The Scatchard method

The binding mode between small molecules with DNA can be determined using the Scatchard procedure. The binding mode between Pr(DNR)$_3$ and DNA

was studied by Scatchard analysis of the fluorescence. The situation was studied in the presence and absence of NaCl in the system (Fig. 11). The Scatchard equation expresses the binding of DNA–AO in the presence of $Pr(DNR)_3$:[24]

$$r_{AO}/c_{AO} = K(n - r_{AO}) \quad (4)$$

where r_{AO} is the moles of AO bound per mole of DNA, c_{AO} is the molar concentration of free AO, n is the binding site multiplicity per class of binding site and K is the intrinsic binding constant of AO with DNA. Thus r_{AO}/c_{AO} *vs.* r_{AO} describes a linear relation. Relevant data and the calculation process of Scatchard plots are given in Table I (as the first line in Fig. 11 without NaCl, for example).

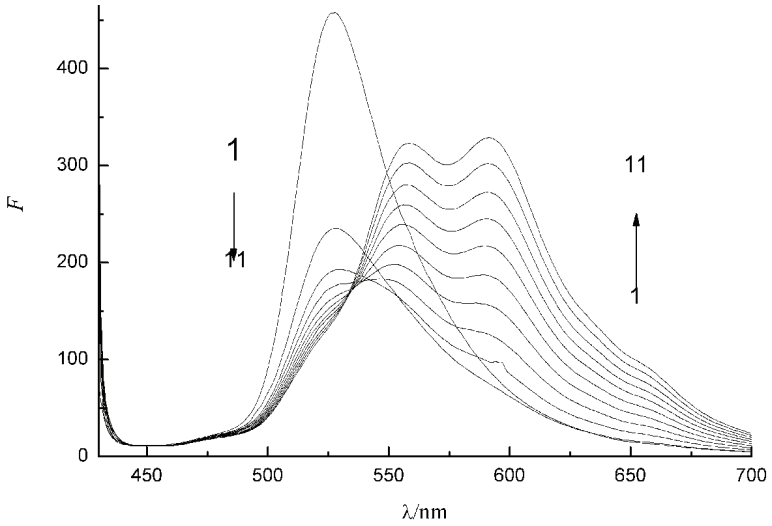

Fig. 10. Influence of $Pr(DNR)_3$ on the emission spectra of AO–DNA; $c_{Pr(DNR)_3} = 1.50\times10^{-4}$ mol L^{-1} (10 μL per scan), $c_{AO-DNA} = 1.00\times10^{-6}$ mol L^{-1}.

Considering the situation in which NaCl was absent from the system, if $Pr(DNR)_3$ interacts with DNA *via* the intercalation mode, the value of n remains constant and that of K changes in the Scatchard plot. If $Pr(DNR)_3$ interacts with DNA through a non-intercalation binding mode involving groove binding or electrostatic interaction, the value of K remains constant while that of n changes in the Scatchard Plot. If $Pr(DNR)_3$ interacts with DNA by mix modes containing non-intercalation and intercalation modes, the value of K and n change in the Scatchard plot.

The Scatchard Graph (Table II) showed that the values of K and n changed in both high concentration and low concentrations. Thus, the mode of interaction between the complex and DNA was a mix mode that was a mixture of intercalation and non-intercalation modes.

To determine whether electrostatic interaction existed, a comparison was made with the system in the presence of NaCl and it was found that increasing the ionic strength reduced the binding number *n*. This showed the existence of electrostatic interaction between $Pr(DNR)_3$ and DNA. The value of *n* may be due to the Na^+ cationic atmosphere surrounding the DNA interfering with the electrostatic interaction by combining with the negative polyphosphate skeleton of DNA and tightening the DNA-chain, so that it becomes difficult for the complex to intercalate in DNA. The results indicated that the major mode of interaction between the $Pr(DNR)_3$ complex and DNA was a combination of electrostatic interaction and intercalation.

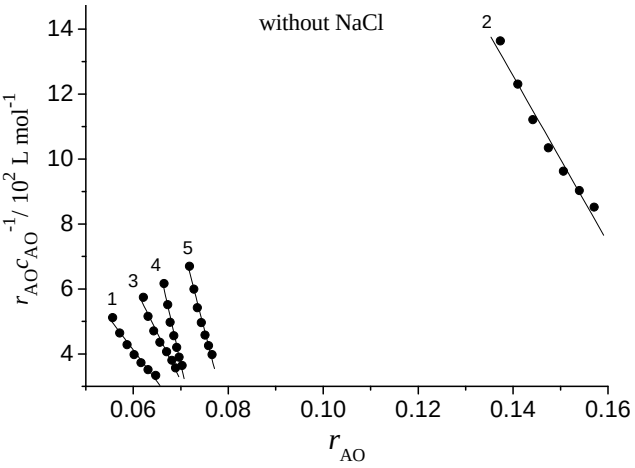

(a)

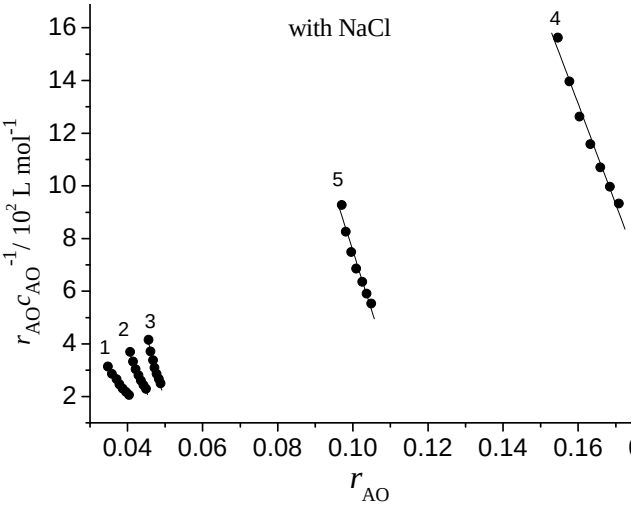

(b)

Fig. 11. Scatchard Plots of $Pr(DNR)_3$–DNA with (a) and without NaCl (b) in different concentrations of AO; c_{DNA} = 1.00×10^{-6} mol L^{-1}; c_{AO} = 4.29×10^{-5} mol L^{-1}; $R_t = c_{Pr(DNR)_3}/c_{DNA}$: 1, R_t = = 0.00, 2, R_t = 0.20, 3, R_t = = 0.40, 4, R_t = 0.60, 5, R_t = = 0.80.

Viscosity method

Optical photophysical probes provide necessary but not sufficient clues to support the nature of the binding modes, whereas hydrodynamic measurements, which are sensitive to length change, are regarded as the most critical tests of a binding model in solution.[25–28] Thus, to further clarify the interaction between $Pr(DNR)_3$ and DNA, viscosity measurements were performed. A classical intercalation model is known to cause a significant increase in the viscosity of a DNA solution due to an increase in the length of the DNA helix. In contrast, a partial or non-classical intercalation mode could bend (or kink) the DNA helix and reduce its effective length and, concomitantly, its viscosity, while non-intercalation binding causes no obvious increase in the viscosity of a DNA solution.

TABLE I. Relevant data and calculation process of the Scatchard plots (as the first line in Fig. 11 without NaCl, for example); $r_{AO} = (c'_{AO} - c'_{AO}(1-F_0/F))/c_{DNA}$; $c_{AO} = c'_{AO}(1-F_0/F)$; c_{DNA} = = 1.00×10^{-6} mol L^{-1}; a, b, c, d, e, f and g are points on the line; c'_{AO} is the initial molar concentration of AO

Parameter	a	b	c	d	e	f	g
F_0/F	0.04864	0.04441	0.04104	0.03826	0.03591	0.03394	0.03232
$1-F_0/F$	0.95136	0.95559	0.95896	0.96174	0.96409	0.96606	0.96768
$c'_{AO}\times10^7$ / mol L^{-1}	11.44	12.87	14.30	15.73	17.16	18.59	20.02
$c_{AO}\times10^7$ / mol L^{-1}	10.8835	12.2985	13.7131	15.1281	16.5438	17.9590	19.3730
$(c'_{AO} - c_{AO})\times10^7$ / mol L^{-1}	0.5565	0.5715	0.5869	0.6019	0.6162	0.6310	0.6470
r_{AO}	0.05565	0.05715	0.05869	0.06019	0.06162	0.0631	0.0647
$r_{AO}c_{AO}^{-1}$ / 10^{-7} mol L^{-1}	0.00511	0.00465	0.00428	0.00398	0.00372	0.00351	0.00334

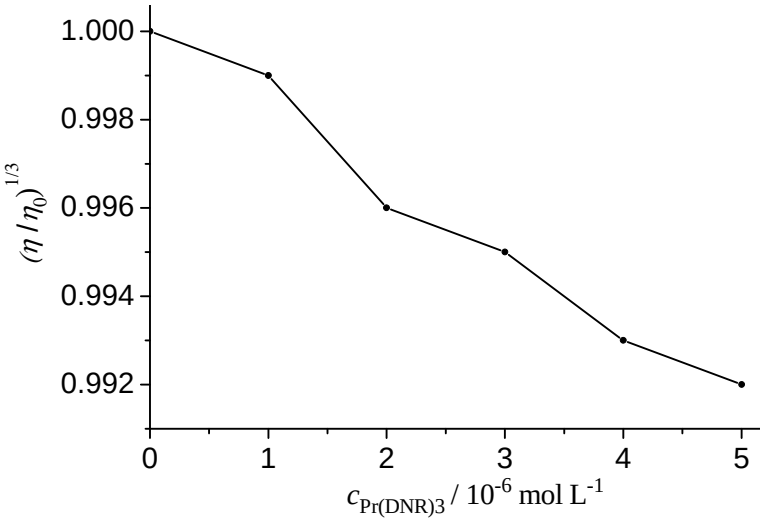

Fig. 12. Effect of increasing amounts of $Pr(DNR)_3$ on the relative viscosities of DNA at 298 K; $c_{DNA} = 1.00\times10^{-5}$ mol L^{-1}.

The changes in the relative viscosity of the DNA solution with increasing concentration of $Pr(DNR)_3$ are shown in Fig. 12. The value of relative viscosity decreased with increasing amount of $Pr(DNR)_3$. Such behavior further suggested that partial or non-classical intercalation binding could be the interaction mode of $Pr(DNR)_3$ with DNA.

TABLE II. Scatchard equation of the interaction between $Pr(DNR)_3$ and DNA

Curve	$R_t = c_{Pr(DNR)_3}/c_{DNA}$	NaCl content, %	Scatchard Equation	K / 10^6 L mol^{-1}	n
1	0.00	5.00	9.72×10^4–1.91×10^6x	1.91	0.0509
		0	1.58×10^5–1.94×10^6x	1.94	0.0814
2	0.20	5.00	1.69×10^5–3.26×10^6x	3.26	0.0518
		0	4.85×10^5–1.94×10^6x	1.94	0.2500
3	0.40	5.00	2.74×10^5–5.12×10^6x	5.12	0.0535
		0	2.40×10^5–2.98×10^6x	2.98	0.0805
4	0.60	5.00	7.41×10^5–3.81×10^6x	3.81	0.1945
		0	4.97×10^5–6.57×10^6x	6.57	0.0756
5	0.80	5.00	5.28×10^5–4.52×10^6x	4.52	0.1168
		0	4.73×10^5–5.68×10^6x	5.68	0.0833

CONCLUSIONS

The interaction between the $Pr(DNR)_3$ complex and hs-DNA was investigated using UV–Vis and fluorescence spectroscopy and viscosity measurements. The obtained results indicated that the binding modes of $Pr(DNR)_3$ to DNA were electrostatic binding and non-classical intercalation binding. The molecular structure of DNR containing an aromatic fused ring plane, which is the internal structure of $Pr(DNR)_3$ can insert into the DNA molecule. However, because of the large volume of the $Pr(DNR)_3$ complex, there was the partial or non-classical intercalation. All these strongly support the idea that the research provides an experimental and theoretical reference for new anticancer drugs.

Acknowledgments. This study was supported by National Natural Science Foundation of China (No. 30973634) and Postgraduate Innovation Foundation of Southwest University of Science and Technology. Mianyang, China.

И З В О Д

МЕХАНИЗАМ ИНТЕРАКЦИЈЕ ИЗМЕЂУ КОМПЛЕКСА PR(DNR)$_3$ И ДНК ИЗ СПЕРМЕ ХАРИНГЕ

XIAOCAI LIU[1], XINGMING WANG[1] и LISHENG DING[2]

[1]*School of Materials Science and Engineering, Southwest University of Science and Technology, Mianyang 62101 и* [2]*Chengdu Institute of Biology, Chinese Academy of Sciences, Chengdu 610041, China*

Испитивање механизма интеракције између лекова и ДНК је важно за разумевање фармакокинетике. У овом раду је анализирана интеракција између комплекса метала ретке земље $Pr(DNR)_3$ и ДНК из сперме харинге у пуферу Tris-HCl (pH 7,4) одређивањем апсорпције, спектра флуоресценције и вискозитета. Резултати су показали да је интеракција између

$Pr(DNR)_3$ и ДНК из сперме харинге електростатичког типа и типа интеркалције. Однос везивања је био $Pr(DNR)_3$:ДНК = 5:1, а константа везивања $K^{\ominus}$(292 K) = $4{,}34\times10^3$ L mol^{-1}. На основу двоструког реципрочног метода и термодинамичке једначине, може се закључити да је интеракција интеркалације била кооперативно контролисана ефектима енталпије и ентропије.

(Примљено 26. августа, ревидирано 8. новембра 2010)

REFERENCES

1. M. Yang, *J. Beijing Med. Univ.* **28** (1996) 303
2. X. M. Wang, H. B .Li, H. P. Liu, Y. M. Hu, L. S. Ding, S. L. Zhao, *Acta Chim. Sinica* **64** (2006) 2115
3. G. F. Cheng, H. Y. Qu, D. M. Zhang, J. D. Zhang, P. G. He, Y. Z. Fang, *J. Pharm. Biomed. Anal*. **29** (2002) 361
4. G. Murphy, W. J. Lawrence, R. Lenhard, *American Society Textbook of Clinical Oncology*, 2nd ed., American cancer society, Atlanta, GA, USA, 1995
5. P. Wiernik, J. Ductcher, *Leukemia* **6 Suppl. 1** (1992) 670
6. X. Q. Chen, Y. Y. Jin, *The Newly Edited Pharmacology*, 14th ed., People's Medicine Press, Beijing, China, 1997, p. 516
7. S. H. Wei, G. S. Liu, *Foreign Medical Sciences, Fascicle*, **26** (1999) 288
8. T. Masahiko, T.-K. Shozo, I. Masamoto, *J. Coord. Chem.* **18** (1988) 77
9. S. Akihiro, O. Takashi, S. Masakatsu, *Tetrahedron* **58** (2002) 75
10. S. I. Dikalov, G. V. Rumyantseva, A. V. Piskunov, L. M. Weiner, *Biochemistry* **31** (1992) 8947
11. P. Zou, *J. Clin. Hematol.* **6** (1993) 78
12. M. Spinelli, J. C. Dabrowiak, *Biochemistry* **21** (1982) 5862
13. S. Mazzini, R. Mondelli, E. Ragg, *J. Chem. Soc., Perkin Trans. 2* (1998) 1983
14. B. B. Hasinoff, K. T. Tran, *J. Inorg. Biochem.* **77** (1999) 257
15. G. X. Xu, *Rare Earths*, Vol. 2, Metallurgy Industry Press, Beijing, China, 1995, p. 451
16. G. X. Xu, *Rare Earths*, Vol. 3, Metallurgy Industry Press. Beijing, China, 1995, pp. 591––597, 606–609, 614
17. X. M. Wang, H. B. Li, Y. M. Hu, D. M. Yang. D. Fei, *Acta Chim. Sinica* **65** (2007) 140
18. P. Yang, C. Q. Zhou, *Acta Chim. Sinica* **61** (2003) 1455
19. S. A. Ysoe, A. D. Baker, T. C. Strekas, *J. Phys. Chem.* **97** (1993) 1707
20. E. J. Gao, S. M. Zhao, Q. T. Liu, R. Xu, *Acta Chim. Sinica* **62** (2004) 593
21. M. Purcell, J. F. Neault, T. Riahi, *Biochim. Biophys. Acta* **1478** (2000) 61
22. A. A. Ouameur, R. Marty, H. A. Tajmir-Riahi, *Biopolymer* **77** (2005) 129
23. Y. Zhang, X. M. Wang, D. Fei, N. Zhao, T. T. Zhao, H. F. Zhu, L. S. Ding, *Chin. Opt. Lett.* **8** (2010) 236
24. P. D. Ross, S. Subramanian, *Biochemistr*y **20** (1981) 3096
25. J. W. Wang, X. P. Zhu, W. Sun, J. G. Xue, Z. X. Wang, M. G. Fu, *Spectrosc. Spectral Anal.* **23** (2003) 899
26. C.A. Mitsopoulou, C. E. Dagas, C. Makedonas, *Inorg. Chim. Acta* **361** (2008) 1973
27. I. H. Bhat, S. Tabassum, *Spectrochim. Acta, A* **72** (2009) 1026
28. C. Y. Chen, K. Chen, Q. Long, M. H. Ma, F. Ding, *Spectroscopy* **23** (2009) 103.